Reactive and Functional Polymers 178 (2022) 105353

Contents lists available at ScienceDirect

Reactive and Functional Polymers

journal homepage: www.elsevier.com/locate/react

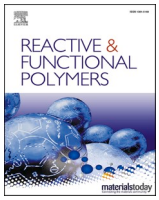

Furan-containing biobased polyurethane nanofibers: A new versatile and green support clickable via Diels-Alder reaction

Stefano Torresi [a], Tamara Calvo-Correas [a], Senda Basasoro [a], Olatz Guaresti [a], Ana Alonso-Varona [b], Nagore Gabilondo [a,*], Arantxa Eceiza [a,*]

[a] Group 'Materials + Technologies', Department of Chemical and Environmental Engineering, Faculty of Engineering of Gipuzkoa, University of the Basque Country UPV/EHU, Spain

[b] Department of Cellular Biology and Histology Faculty of Medicine and Odontology, University of the Basque Country UPV/EHU, Spain.

ARTICLE INFO

Keywords:
Click chemistry
Nanofibers
Biobased polyurethane
Green chemistry

ABSTRACT

A new biobased polyurethane formulation containing furan was synthesized and subsequently functionalized and de-functionalized via Diels-Alder and retro Diels-Alder reactions. Furan was inserted in the backbone polymer using 2,5-bis(hydroxymethyl)furan as chain extender. At the same time, another composition not containing furan was synthesized as reference. Both formulations were produced initially as films and then processed using electrospinning to obtain nanofibers membranes. The absence of catalysts, the high renewable content, the facile synthesis and spinnability of the polymer allow a quantitative and green production of versatile functionalizable platforms. The kinetic and efficiency of the functionalization were assessed using two different compounds: Fluorescein-5-maleimide and 3-Maleimidopropanoic acid. The high hydrophobicity of the membranes permits to perform the functionalization reactions in water, resulting in a process that minimally affects the membrane integrity which is, at the same time, environmental-friendly. Finally, the good biocompatibility opens the way for its use as biomedical tissue, widening the range of possible application of this material.

1. Introduction

In the last years, nanomaterials have been intensively investigated, due to their improved properties with respect to their homologues at the macroscale. Physical, biological and chemical properties are affected by the increased surface area both to volume and mass ratios.

Among nanomaterials, the last advances in the electrospinning process boosted the research regarding nanofibers. Indeed, this technique allows the fast and easy production of a large quantity of high-quality nanofiber. Furthermore, a wide range of fiber diameters (from nanometers to micrometers) could be produced by adjusting the electrospinning parameters and more than a hundred of polymers as well as inorganic materials have been electrospun [1], thus confirming the huge versatility of this technique.

Nanofibers have a great variety of applications and new ones are discovered constantly. The reduced porosity of the electrospun nanofibers membranes, with pore size typically in the submicron range, make them a perfect material for filters and microfilters [2]. Additionally, nanofibers find important applications is the tissue engineering as the morphology of nanofibers scaffolds resemble the natural extracellular matrix, thus creating a biomimetic cellular environment [3]. Electrospun nanofibers are also used in sensing, energy conversion, catalysis, wound healing, storage devices and biomolecular immobilization, to mention but a few [1].

As the research in polymer chemistry has switched to sustainable materials, biobased nanofibers have also started to be thoroughly investigated. For example, chitosan-based nanofibers membranes have been produced for being applied as arsenic removers [4] and biopolyurethane nanofibers, containing a polycaprolactone/castor oil hybrid polyol, have been functionalized by triclosan-cyclodextrin

Abbreviations: CuAAC, copper-catalyzed azide-alkyne cycloaddition; DA, Diels-Alder; r-DA, retro Diels-Alder; NMR, Nuclear magnetic resonance; FTIR, Fourier transform infrared spectroscopy; DSC, differential scanning calorimetry; TGA, thermo gravimetric analysis; SEM, scanning electron microscopy; WCA, static water contact angle; PBSD, Poly(butylene sebacate)diol; HDI, 1,6-Hexamethylene diisocyanate; BHMF, 2,5-Bis(hydroxymethyl)furan; PD, 1,3-Propanediol; 5-MF, Fluorescein-5-maleimide; MPA, 3-Maleimidopropanoic acid; DMF, *N*,*N*-Dimethylformamide; $CHCl_3$, chloroform; DMSO, dimethyl sulfoxide; MEM, Minimum essential medium; HS, hard segment; DTG, derivative of thermogravimetric curve; UV–vis, Ultraviolet-visible.

* Corresponding authors.
E-mail address: arantxa.eceiza@ehu.eus (A. Eceiza).

https://doi.org/10.1016/j.reactfunctpolym.2022.105353
Received 2 May 2022; Received in revised form 5 July 2022; Accepted 12 July 2022
Available online 14 July 2022

complexes in order to increase their antibacterial properties [5].

Indeed, the high area to volume ratio dramatically increases the ease of functionalization of the nanofibers, thus allowing to go beyond the classical polymer functionalization methods such as plasma and wet chemical treatment or surface graft polymerization, which are resource-consuming processes [6]. In this sense, click reactions are modular, providing high reaction yields and producing none or inoffensive byproducts, in accordance with the principles of green chemistry. Consequently, in the last years they have come up as efficient chemical tool for post-polymerization functionalization [7]. The great variety of reactants and click reactions that can be involved allow to create nanofibrous platforms ready for being functionalized and which can be used in a wide range of applications.

For instance, copper-catalyzed azide-alkyne cycloaddition (CuAAC) reaction has been used to immobilize testis-specific protease 50 on a polymer substrate to create a biomarker-functionalized platform for breast cancers diagnosis [8], while thiol-ene click reaction has been employed to attach maleimide terminated PNIPAM to poly((3-mercaptopropyl)methylsiloxane), which contains free sulfur groups, in order to produce thermo-sensitive fibers [9].

Another relevant reaction belonging to the select click chemistry group is the Diels-Alder cycloaddition (DA). In organic chemistry, it is widely used for the diastereo- and regioselective generation of six-membered rings with up to four stereogenic centers [10]. Moreover, it has been used in different surface modification processes [11,12]. In this [4 + 2] cycloaddition reaction, a diene and a dienophile undergo a direct reaction (DA) and, afterwards, a retro (r-DA) reaction, once increased the temperature. The thermo-reversibility of DA perfectly fits the requirements for self-healing and recyclability of polymers, as demonstrated by the great quantity of studies carried on these topics [13–17].

In this work two different polyurethanes, one bearing a furan-containing chain extender which can be functionalized by DA reaction and another using not clickable commercial 1,3-propanediol chain extender as reference, were synthesized and characterized. Films and membranes of electrospun nanofibers were produced. The two formulations were characterized both as film and as membrane using nuclear magnetic resonance (NMR), Fourier transform infrared spectroscopy (FTIR), Gel Permeation Cromatography (GPC), differential scanning calorimetry (DSC), thermo gravimetric analysis (TGA), tensile test, scanning electron microscopy (SEM), static water contact angle (WCA) and cytotoxicity test. The effect of furan groups on the polymer properties and the influence of the different processing method on the final properties of the obtained material were evaluated. Finally, the occurrence of the Diels-Alder reaction on the furan-containing electrospun nanofiber membrane was verified by UV light tracking of clicked maleimide containing fluorescent label. Subsequently, the DA and r-DA reaction on the membrane were followed using UV–vis spectroscopy.

2. Materials and methods

2.1. Materials

Poly(butylene sebacate)diol (PBSD) derived from castor oil was used as macrodiol. The hydroxyl index, determined by titration with ASTM D 4274–88 Test Method A was 32.01 mg KOH g^{-1} and the number average molecular weight was 3505 g mol^{-1}. The biobased carbon content of PBSD was 72% according to the ASTM-D6866-12 (0.98) Method B (AMS) standard procedure [18]. 1,6-Hexamethylene diisocyanate (HDI, 168 g mol^{-1}) was kindly provided by Covestro AG. 2,5-Bis(hydroxymethyl)furan (BHMF, 128 g mol^{-1}), a biobased furan-containing heterocyclic organic compound and 1,3-propanediol (PD, 76 g mol^{-1}) used as chain extender were purchased by Apollo Scientific Ltd. and Quimidroga S.A., respectively. The labelling agent Fluorescein-5-maleimide (5-MF, 427 g mol^{-1}) was purchased by Tokyo Chemical Industry Co., Ltd., while 3-Maleimidopropanoic acid (MPA, 169 g mol^{-1}) was synthesized following previously reported procedure [19]. *N,N*-Dimethylformamide (DMF) and chloroform ($CHCl_3$) were purchased by Scharlau, while dimethyl sulfoxide (DMSO) by Macron Fine Chemicals. Minimum essential medium (MEM), non-essential amino acids and sodium pyruvate were purchased by Gibco. Penicillin and streptomycin were provided by Lonza and fetal bovine serum by HyClone.

All the products were used as received except for macrodiol, which was dried under vacuum at 80 °C for 4 h prior to use.

2.2. Synthesis of polyurethanes

The polyurethanes were synthesized using a two-step or prepolymer bulk polymerization method. Firstly, dried PBSD and HDI were added to a two necked round flask, purged with N_2, mechanically stirred at 90 rpm and made react at 90 °C for 2 h. Then the chain extender (BHMF or PD) was added to the prepolymer and after mixing for 5 min, the viscous liquid was transferred to a mold and pressed at 50 bar at 100 °C for 10 h to complete the polymerization. No catalyst was used. Films of 170 mm long, 170 mm wide and 1.4 mm thick were produced.

The same components equivalent ratio was employed in the synthesis of both PBSD:HDI:PD and PBSD:HDI:BHMF compositions, which was 1:3:2. Samples were named as PU-PD and PU-BHMF according to the chain extender employed. The hard segment (HS) content of PU-PD and PU-BHMF, calculated as the weight percentage of diisocyanate and chain extender, were 16 and 18 wt%, respectively. The polyurethane synthesis is depicted in Scheme 1.

2.3. Electrospinning of synthesized polyurethanes

Prepared films were cut in small pieces and dissolved in a closed vial in a DMF:$CHCl_3$ mixture (2:1 *v*/v) for 12 h under constant stirring at 50 °C, thus obtaining a homogenous solution.

Different polyurethane weight percent ranges were tested, 11–13 wt % for PU-PD and 12–15 wt% for PU-BHMF, in order to select the best concentration for each composition. Voltage, flow rate and distance from the syringe needle to the collector were also optimized. The best conditions for producing defect-free nanofibers in a long-lasting continuous electrospinning process for both compositions were found to be 9 kV, 0.5 mL h^{-1} and 15 cm, respectively. The membranes were produced collecting the electrospun nanofibers on aluminum foil for 90 min following by a drying step at room temperature for 12 h.

2.4. Electrospun membranes functionalization through Diels-Alder reaction

As previously mentioned, furan and maleimide derivatives efficiently undergo DA reaction. Herein, furan-containing polyurethane nanofibers were functionalized with two different maleimide-containing compounds via DA reaction. DA occurrence was assessed by observing the membranes functionalized with 5-MF under UV light at 365 nm. Firstly, 2 mg of 5-MF were dissolved in 6 mL of H_2O:DMSO in a 3:1 volume ratio and vigorously stirred at 65 °C for 24 h until complete dissolution. Subsequently, the PU-BHMF membrane was added and maintained at 65 °C for 24 h. After that, the membrane was removed and repeatedly washed in the same solution of H_2O:DMSO to remove the unreacted 5-MF.

Besides, the DA was also reacting PU-BHMF with MPA in neat water. In a closed vial, was letting evolve, at 60 °C, an equimolar amount of furan and maleimide groups. The DA reaction was monitored by UV–vis spectrometry taking aliquots from the reaction medium at different times. Finally, the r-DA was performed at 120 °C during 3 h until the complete release of MPA, which was confirmed by UV–vis spectroscopy.

2.5. Characterization

Proton nuclear magnetic resonance (^{1}H NMR) spectra of

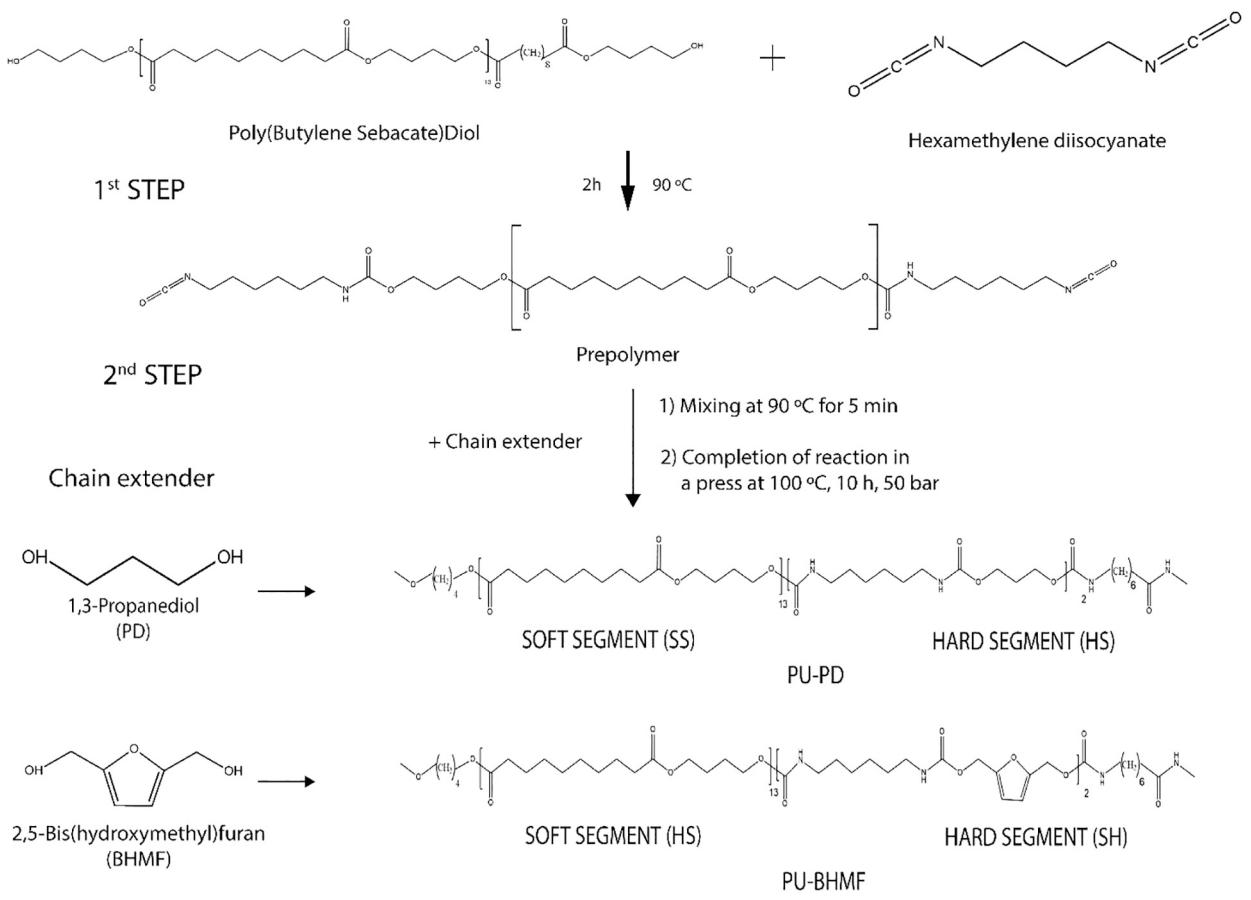

Scheme 1. Scheme of polyurethanes' synthesis

polyurethanes were recorded to confirm the incorporation of furan groups in the polyurethane chain using a Bruker Avance Neo 500 NMR spectrometer at resonance frequency of 500 MHz. Deuterated chloroform was used as solvent.

Polyurethanes were also characterized using Fourier transform infrared spectroscopy. The spectra were recorded performing 32 scans with a resolution of 4 cm^{-1} using a Nicolet Nexus spectrometer equipped with a MKII Golden Gate accessory (Specac) involving a diamond crystal at a nominal incidence angle of 45° and ZnSe lens. The spectra were recorded between 4000 and 650 cm^{-1}.

The polyurethanes were also characterized in terms of weight average molecular weight (Mw), number average molecular weight (Mn) and polydispersity index (PDI), determined by gel permeation cromatography (GPC) using a Thermo Scientific chromatograph equipped with an isocratic Dionex UltiMate 3000 pump and a RefractoMax 521 refractive index detector. The separation was carried out at 30 °C within four Phenogel GPC columns from Phenomenex, with 5 μm particle size and 10^5, 10^3, 100 and 50 Å porosities, respectively, located in an UltiMate 3000 Thermostated Column Compartment. The mobile phase was THF at a flow rate of 1 mL min^{-1}. The polyurethanes were dissolved in THF at 1 wt% and filtered using 2 μm pore size nylon filters. Results were reported to as weight average monodisperse polystyrene standards.

The thermal behavior of the synthesized polyurethanes was investigated using differential scanning calorimetry (DSC)3+ Mettler Toledo. Samples with a weight between 5 and 10 mg were sealed in aluminum pans and heated from −75 to 220 °C at a constant heating rate of 30 °C min^{-1}. The inflexion point of the heat capacity was chosen to evaluate the glass transition temperature, Tg. Melting temperature (Tm) was settled as the maximum of endothermic peak taking the area under the peak as melting enthalpy (ΔHm).

Thermogravimetric analysis (TGA) was performed in order to assess the thermal stability of both polyurethanes. The analysis was performed using a TGA/DSC3+ Mettler Toledo equipment. Samples were heated from 25 to 800 °C in a nitrogen atmosphere at a constant rate of 10 °C min^{-1}. The initial degradation temperature was assumed as the point where 5% of the total weight was lost while the maximum degradation temperature was taken as the minimum peak in the derivative of thermogravimetric curve (DTG).

Mechanical behavior was evaluated using an Instron 5967 testing machine provided with a 500 N load cell. Dog-bone shaped specimen were punched from polyurethane films. Pneumatic grips of 1 kN were used to hold the sample. The test was performed at a crosshead rate of 50 mm min^{-1} using 500 kN load cell.

Data from four specimen of each sample were averaged to obtain the elastic modulus E, ultimate tensile strength (σ_t), and elongation at break (ε_b).

The morphology of the electrospun nanofiber membranes was analyzed with a Hitachi S-4800 scanning electron microscope (SEM), at 5 kV accelerating voltage. The diameter distribution was calculated on six different images for each electrospun membrane using ImageJ software.

Static water contact angle measurements (WCA) were performed using a SEO-Phoenix-300-Touch in order to evaluate the surface properties of both films and electrospun mats.

A drop of 4 μL of deionized water was deposited on the surface of the films and the membranes. To obtain a perfectly flat surface, the membrane was directly obtained by electrospinning on a blank microscope slide attached to the collector. Three different measurements on two different sample of each polyurethane film and membrane were performed and averaged to obtain the contact angle values. The images were processed using Surfacewear 8 software.

The cytotoxicity was determined following the ISO 10993-5:2009, using L929 mouse fibroblast cells. As complete medium was used MEM with an addition of 1% non-essential amino acids, sodium pyruvate 1 mM, 100 U ml^{-1} of penicillin and streptomycin plus a 10% of bovine fetal serum. The extracted culture medium was prepared following the ISO 10993-12:2012, immersing sterilized samples of PU-PD and PU-BHMF in complete medium at 37 °C for 24 h.

L929 cells were seeded on Sarstedt 96-well cell culture plate at a density of 4×10^3 cells/well and incubated at 37 °C for 24 h. Each well was filled with L929 cells and 100 μL of complete medium.

A blank (complete medium without cells), negative (complete medium with cells) and positive (complete medium and 10% of DMSO) controls were prepared. After the incubation time of 24 h at 37 °C the complete medium was substituted by extractive medium.

The viability was determined using the PrestoBlue™ cell viability reagent. The absorbance at 570 nm and 600 nm was measured using a microplate reader. and mean values and their standard deviations were calculated.

Viability (%) was calculated as follow:

$$Viability\ (\%) = \frac{A_{test}}{A_{control}} \times 100$$

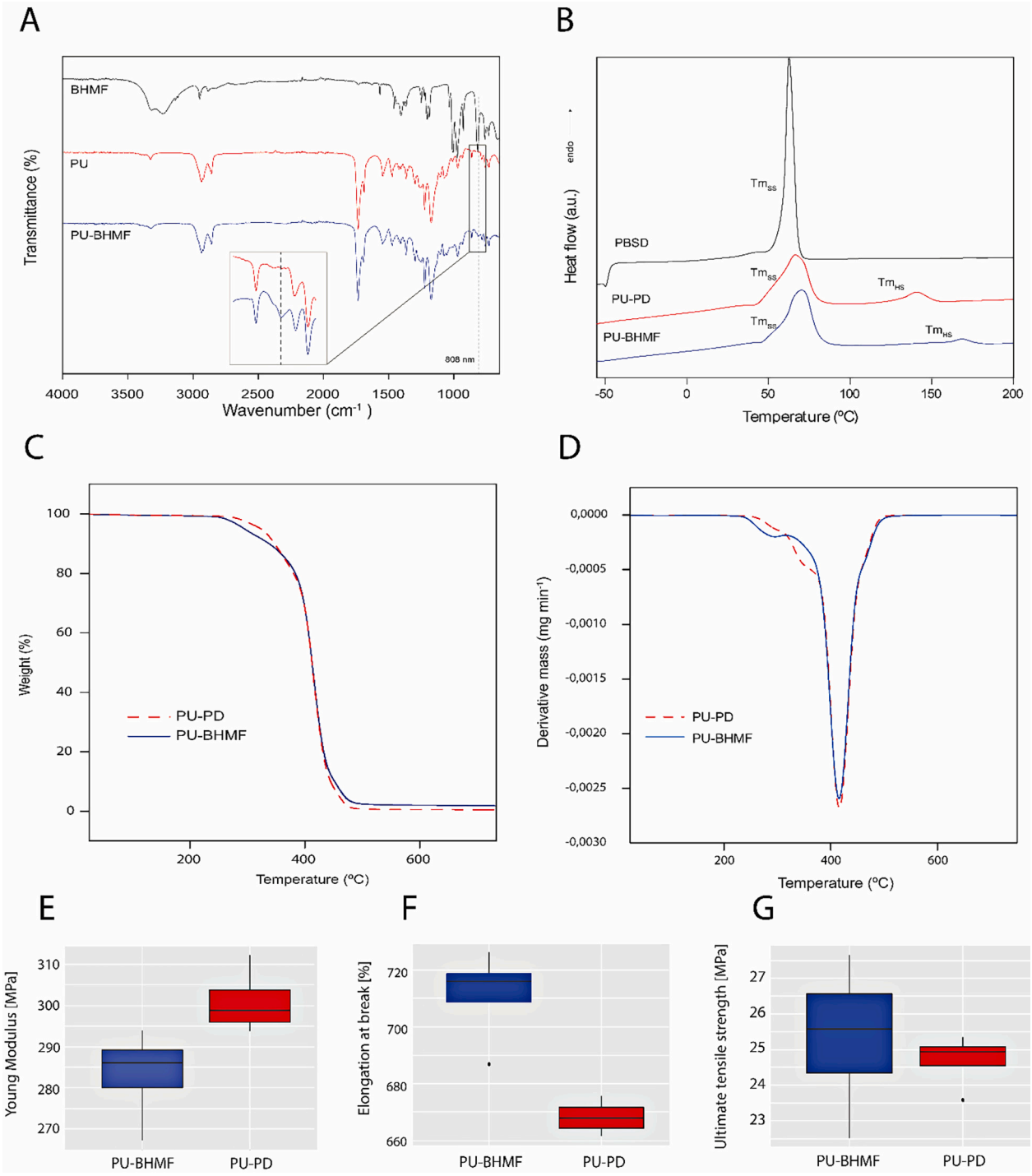

Fig. 1. A) FTIR spectra of BHMF, PU-PD and PU-BHMF; B) DSC thermograms of the two synthesized polyurethanes and pure polyol; C) Variation of the weight loss; D) derivative of the weight loss of PU-PD and PU-BHMF E), F) and G) Mechanical properties of the two polyurethanes.

where A_{test} is the absorbance of the sample cells and $A_{control}$ is the absorbance of the negative control cells.

The occurrence of DA reaction between PU membranes and the fluorescent marker (5-MF) was corroborated by observing functionalized membranes under UV light at λ_{max} = 365 nm. Ultraviolet-visible (UV–vis) spectroscopy was used to monitor the DA reaction between PU-BHMF and MPA in water using a Shimadzu UV-3600. Spectra were collected at the beginning and at different times during the reaction.

3. Results and discussion

3.1. Physicochemical and mechanical characterization of polyurethanes

The chemical structure of the two synthesized polyurethanes was analyzed by ^{1}H NMR, in order to confirm the presence of furan in PU-BHMF backbone. Fig. S1 shows the spectra of the two formulations, the chemical structure of synthesized polyurethanes and the assignment of the peaks. For BHMF chain extender, characteristic peaks can be identified at 6.3 and 5.0 ppm corresponding to the H of furan ring (Hl) and to the H of methylene group (Hi), respectively [20].

Further confirmation of BHMF's presence in the polymer backbone is given by the integral value of the signal at 5.0 ppm, being double with respect the one at 6.3 ppm, matching the theoretical predictions. The ratio of PBSD:HDI:PD and PBSD:HDI:BHMF was calculated from the spectra by the correlation of the measured areas of the protons of the methylene peak of PBSD (2.3 ppm, labelled as c in the graph) and methylene group of HDI (1.5 ppm, labelled as g in the graph) (Fig. S1). The total number of methylene moieties contributing to the c signal of the PBSD was calculated from its ^{1}H NMR spectrum, referring it to chain end methylene group (3.7 ppm, labelled as m in the graph), which revealed a polymerization degree (n) of 13 (Fig. S2). The obtained values are 1:3.1:2.2 and 1:2.9:1.9 for PBSD:HDI:PD in PU-PD and for PUBD:HDI:BHMF in PU-BHMF, respectively, which are similar to the theoretical ratio of 1:3:2. FTIR analysis was used to analyze the characteristic functional groups of the synthesized polyurethanes as well as to confirm the presence of furan groups in PU-BHMF. The spectra of BHMF chain extender and the synthesized polyurethanes are shown in Fig. 1A. As it can be observed, the FTIR spectra of both polyurethanes are similar. The peak corresponding to the stretching vibration of isocyanate at 2270 cm^{-1} is absent in both polyurethane formulations, thus confirming that all the isocyanate reacted during the synthesis. On the other hand, the synthesized polyurethanes showed several bands characteristic of the urethane group, the N—H stretching vibration around 3320 cm^{-1}, the C═O stretching vibration at 1730 cm^{-1}, the C—N stretching vibration combined to N—H out-of-plane bending at 1540 cm^{-1} and the CO—O stretching vibration at 1170 cm^{-1} [21].

However, the peak at 808 cm^{-1} corresponding to the C—H wagging of a trisubstituted alkene is present only in PU-BHMF, confirming the incorporation of furan moieties in PU-BHMF [22].

The resulting Mn and Mw for PU-PD were 35,374 g mol^{-1} and 65,989 g mol^{-1} respectively, resulting in a PDI of 1.86, while for PU-BHMF Mn and Mw were 31,857 g mol^{-1} and 61,166 g mol^{-1} respectively, with a PDI of 1.92. The obtained values confirm that the synthesis was performed successfully.

The thermal behavior of the synthesized polyurethanes was analyzed by DSC. Fig. 1B shows the thermograms of PU-PD and PU-BHMF, as well as that of the neat macrodiol. The main thermal transitions related to both hard and soft segments of PU-PD and PU-BHMF polyurethanes can be observed in thermograms. The peak around 60 °C, also present in the castor oil derived PBSD macrodiol, is assigned to the melting of the soft segment, TmSS. Besides, the transition observed at higher temperature, at 130 °C for PU-PD and 170 °C for PU-BHMF is associated with the melting of hard segment, TmHS, and it is clearly influenced by the chain extender chemical structure. Thus, the use of a chain extender with symmetrically di-substituted furan-ring resulted in higher melting temperature of the hard segment. However, despite its higher TmHS value, PU-BHMF shows lower crystallinity than PU-PD as deduced from their melting enthalpy values (1.82 vs 8.02 J g^{-1}), since steric hindrance of BHMF hinders hydrogen bonding interaction and, hence, the formation of inter-urethane interaction among chains. Similar behavior was observed in the literature when comparing hard segments with different, aliphatic or aromatic, symmetric diisocyanate types [23,24]. Thermal degradation of synthesized polymers was investigated using TGA (Fig. 1C). Both polyurethanes showed a first degradation step related to the hard segment and a second one related to the soft segment [25]. The first degradation peak of PU-BHMF appeared around 285 °C, similar to other furan-based polymers [20,26]. In the case of PU-PD, the first degradation peak was split in two different peaks, both at higher temperature than the PU-BHMF's one. The observed better thermal stability of PU-PD is attributable to the higher crystallinity degree deduced by the DSC measurements. The second peak, not depending on the type of chain extender used, occurred at the same temperature in both polyurethanes and it is attributed to the soft segment degradation resulting in the decomposition of polyol main chain with a shoulder at higher temperature due to degradation of the carbonaceous residues.

Mechanical properties of polyurethanes are closely related to their composition and microstructure. In general, the hard segment acts as physical crosslinking region and imparts stiffness to the polyurethane, whereas the soft phase, due to the long linear structure of the macrodiol, imparts flexibility to the material. The values obtained for Young's modulus, elongation at break and ultimate tensile strength are gathered in Fig. 1E, F and G, respectively.

As it could be noted, comparable values were obtained for both polyurethanes, suggesting that properties are mainly governed by the macrodiol, which is the same in both polyurethanes and whose content is greater than 80 wt%. However, slightly higher elastic modulus value was measured for PU-PD, which can be attributed to its higher crystallinity degree in the hard segment, in agreement with DSC results. Both polyurethanes showed high ductility, being slightly higher for PU-BHMF according to its lower crystallinity.

3.2. Electrospun polyurethane membranes characterization

The goal of the work was not only the synthesis and characterization of a new furan-containing biobased polyurethane but also the production of functionalizable nanofiber platforms. With that purpose, electrospun membranes were successfully prepared from both polyurethanes. It has to be taken into account that the clickability of the supports could be hindered by the fact that the furan moieties are in the backbone chain, thus being less reactive than side chain moieties. However, the high surface area to volume ratio of nanofibers would compensate this drawback, resulting in, as it will be showed, fast and easily functionalizable nanofibers.

The morphology and size of electrospun nanofibers were analyzed by SEM as shown in Fig. 2A and B. It can be observed that both PU-PD and PU-BHMF samples exhibit a suitable spinnability resulting in beadless and morphologically homogenous nanofibers. The best quality nanofibers were achieved at 11 and 13 wt% solution concentration for PU-PD and PU-BHMF, respectively. Marked difference in the diameter of the nanofibers is easy to notice, measuring 500 ± 102 nm mean diameter of PU-PD and 1184 ± 273 nm that of PU-BHMF one's, probably due to the different concentration employed for the solutions. However, the obtained diameters were similar to those of others clickable polyurethane nanofibers [12,27,28], and, moreover, different diameters could be produced changing the process parameters.

The surface properties of electrospun membranes were assessed by water contact angle measurements (WCA). For comparative purpose, the WCA of both films and membranes was measured (Fig. 2). PU-PD and PU-BHMF films showed a WCA of 77 and 66°, respectively, while in the case of the membranes, WCA was 120 and 125°, respectively. In order to explain the difference in the films' WCA, the solubility parameters (δ) of the PU-PD hard segment (δ_{PD} = 22.2 J$^{1/2}$ cm$^{-3/2}$), PU-BHMF hard

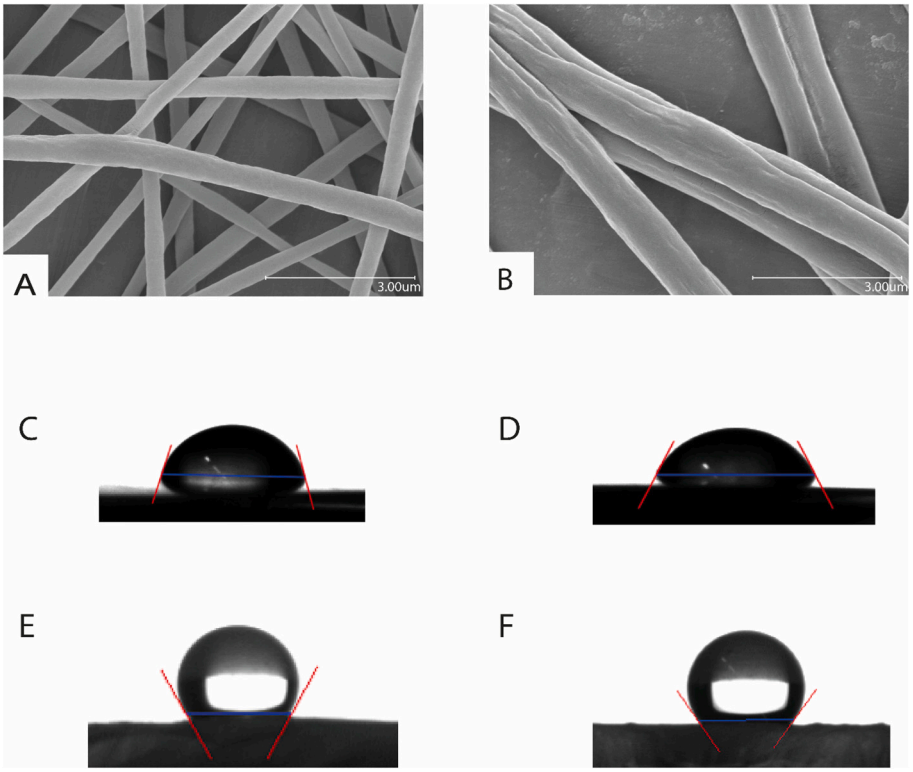

Fig. 2. SEM images of A) PU-PD and B) PU-BHMF electrospun nanofibers produced under the following voltage, flow rate and distance between the syringe needle to collector conditions: 9 kV, 0.5 m h-1, and 15 cm; water contact angle images of C) PU-PD and *D*) PU-BHMF films and E) PU-PD and F) PU-BHMF nanofibers membranes.

segment (δ_{BHMF} = 23.5 $J^{1/2}$ $cm^{-3/2}$) and PBSD soft segment (δ_{PBSD} = 19.3 $J^{1/2}$ $cm^{-3/2}$) were calculated using the Hoftyzer-Van Krevelen method. It can be noticed that the PU-BHMF hard segment is less miscible in PBSD than PU-PD hard segment, since the Δδ between soft and hard segments is higher. This implies that in the PU-BHMF formulation urethane domains form stronger and more segregated dipoles, which result in lower WCA values. As reported in literature, the electrospun membranes possess high roughness which implies a high WCA value [29].

The high hydrophobicity of the membranes permits to perform the functionalization in water without affecting the membrane integrity, thus resulting in a process that minimally affects the membrane integrity which is, at the same time, environmental-friendly.

In vitro biocompatibility of PU-PD and PU-BHMF membranes was evaluated by short–term cytotoxicity and cell adhesion assays. As mentioned, the cell viability was measured incubating L929 murine fibroblast cells for 24, 48 and 72 h in PU-PD and PU-BHMF membranes extracted medium. The proliferation curve (Fig. 3A) showed similar pattern to that obtained for negative control, even higher for the first 48 h, showing an increasing proliferative kinetic. For the entire duration of the experiment, the viability (Fig. 3B) remained well above the 70% of acceptance limit set down by ISO 10993-5 standard [30], denoting a non-toxic behavior. The adhesion of cells to PU-PD and PU-BHMF membranes was analyzed by SEM (Fig. 3C). It can be seen that cells are well adhered to the surface, acquire a flattened morphology and present numerous cytoplasmic projections, covering the surface of materials at 72 h, that allows stable cell adhesion. Taking into account the obtained biocompatibility preliminary results, the prepared electrospun PU-PD and PU-BHMF membranes open the path for future studies regarding the use of these materials as biomedical devices.

3.3. DA functionalized electrospun membranes characterization

The efficiency of conjugation strongly depends on the physical state of polymers. During functionalization reactions, polymers in solution act in a different manner with respect to heterogeneous surfaces [31]. In order to assess the possibility to perform the DA click reaction on heterogeneous surface, as in the case of the developed electrospun membranes, the maleimide bearing 5-MF fluorescent marker was used. This compound is mainly employed as protein labeling agent, [32] by the thiol-Michael addition reaction, but it can also be used as marker for DA cycloaddition, once it reacts with furan moieties [17]. The functionalization reaction was performed on both PU-PD and PU-BHMF membranes. It was tried also on PU-PD, even if it did not contain furan moieties, in order to exclude the possibility that 5-MF remained just physically trapped in between the membrane's pores. After the reaction times, the membranes were analyzed under UV light at 365 nm. Fig. 4 shows a digital image of irradiated PU-BHMF and PU-PD membranes taken after the treatment with 5-MF.

As it can be clearly noticed, PU-BHMF showed homogeneous fluorescence demonstrating the successful functionalization of the nanofibers whereas, PU-PD did not present fluorescence at all.

Once assessed the possibility to perform DA click reaction on the membrane, MPA was used to monitor the reaction by UV–vis spectroscopy. MPA was chosen because it results easier to handle with respect to 5-MF and, at the same time, it allows to perform the DA reaction in aqueous solutions thus opening the possibility to functionalize the membrane with bioactive molecules, which is otherwise prevented due to toxicity concerns. Fig. 5A shows the evolution of UV spectrum during the functionalization of the PU-BHMF membrane at 60 °C. As it can be observed, MPA showed the absorption peak near 270 nm in aqueous solutions. The reduction of the absorption peak of MPA, given by the loss of conjugation of maleimide, would indicate the consumption of MPA due to the formation of the DA adduct [17]. An equimolar amount of

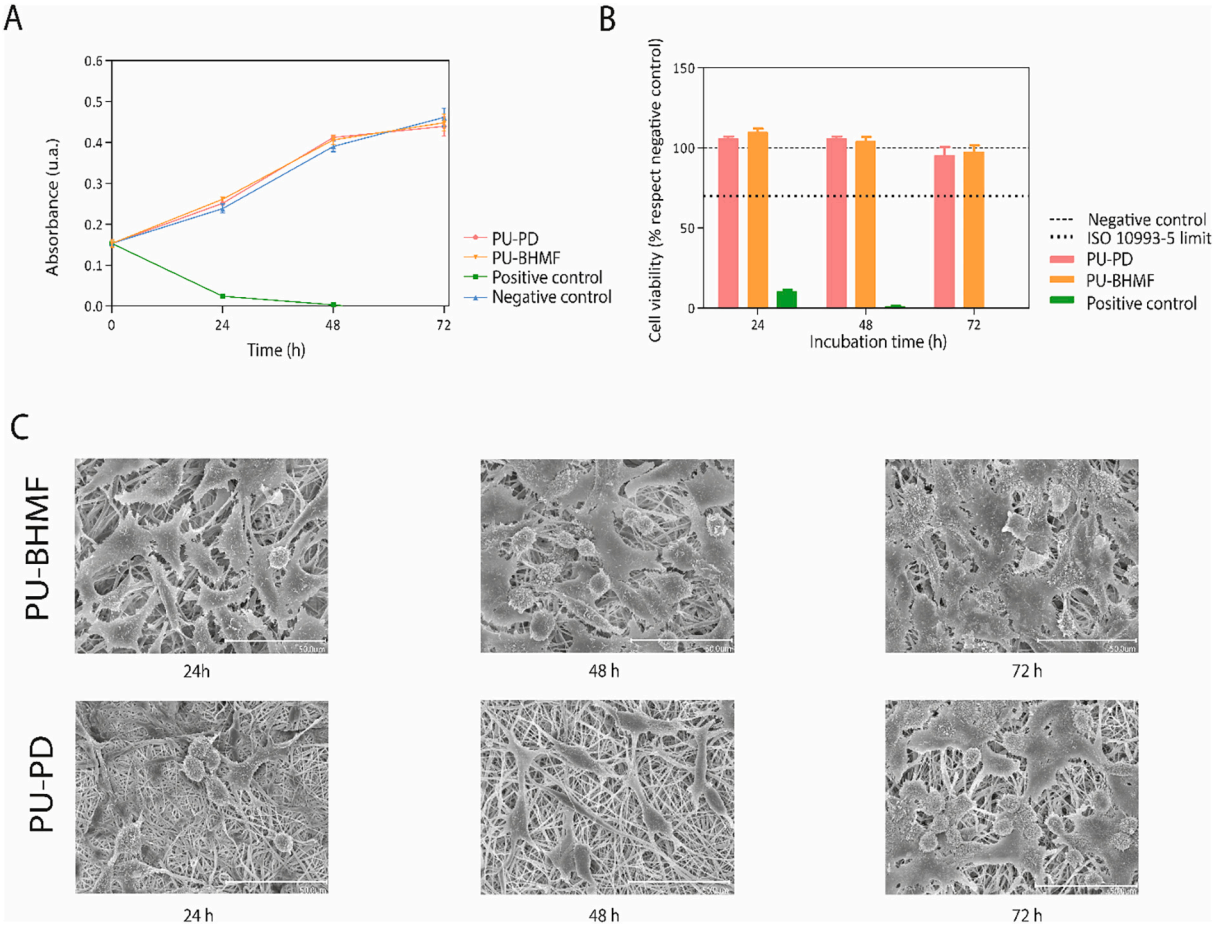

Fig. 3. In vitro biocompatibility of PU-PD and PU-BHMF: A) proliferation curve; B) cell viability and C) cell adhesion at different times.

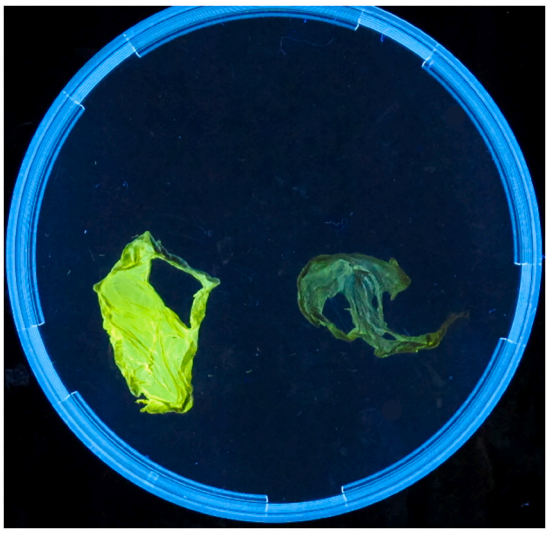

Fig. 4. PU-BHMF (left) and PU-PD (right) membranes after treatment with 5-MF under UV light at 365 nm.

maleimide and furan groups were allowed to react. The PBSD:HDI:BHMF ratio in the membrane was considered to be 1:3:2, as it was corroborated by ^{1}H NMR. Briefly, 90 mg of PU-BHMF membrane (0.03 mmol of furan) were incubated in 6 mL of 0.005 M MPA aqueous solution (0.03 mmol of maleimide). The efficiency of the functionalization was calculated as 49% (Fig. S3). As it can be observed, the maleimide consumption was practically completed within 2 h, coherently with other studies reported in the literature [33,34]. Indeed, the largest amount of maleimide, corresponding to the greatest decrease in UV–vis peak, reacted in the first 30 min. Then, during the next 2 h, just a negligible peak decrease occurred.

This high reaction rate could be ascribed to the high surface area of the nanofibers, which results in an easy accessibility to the furan moieties. However, it should be mentioned that different membranes pieces gave different kinetics due to the difficult control over the membrane in terms of thickness, roughness and nanofibers accessibility. One interesting feature of the DA reaction is that the r-DA can be thermally achieved at relatively low temperature [35]. Once the coupling between the accessible furan groups of the membrane and the maleimide group of MPA to the DA adduct formation was corroborated, the functionalized membrane was heated up to 120 °C for the decoupling of the DA reactants. Fig. 5B shows the UV–vis spectra for the r-DA reaction. Increasing the temperature, indeed, the equilibrium is shifted towards the production of the DA precursors, i.e., furan and maleimide, and it results in the increase of the absorbance peak. As can be seen, the r-DA reaction occurred in 180 min. It is also noticeable that the peak is shifted to lower wavelengths which could be ascribed to nanofiber morphology modification due to the high temperature reached during the process, much higher than the Tm of the soft segment.

Taking into account the thermoreversibility of the DA reaction, a second DA reaction was performed on the same membrane after the r-DA to confirm the possibility of multiple subsequent functionalization and de-functionalization cycles [S2]. The second DA showed similar kinetic to the first DA. In order to ensure that the maleimide was in fact reacting with the furan groups of the PU-BHMF membrane and not just

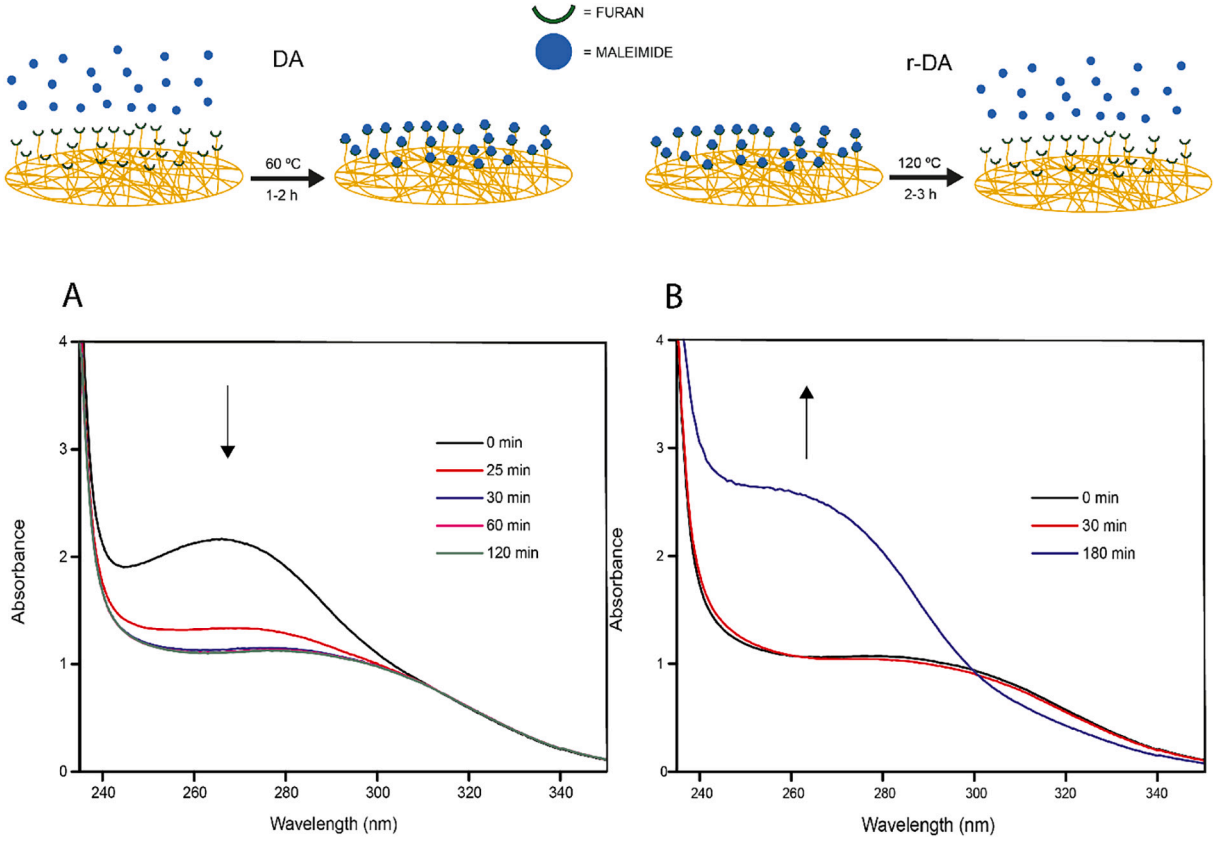

Fig. 5. Scheme of functionalization and de-functionalization reactions over the membrane and UV–vis absorbance variation during: A) DA and B) r-DA using AMI as dienophile.

being trapped between the membrane's pores, PU-PD membrane underwent the same process. In this case, no changes in the absorbance spectra were registered and the graph of this reaction is deliberately omitted.

4. Conclusions

A new biobased polyurethane with high content of renewable components has been synthesized without the need of catalysts. The new polymer has been characterized and then electrospun using electrospinning to obtain good quality nanofibers. Thanks to the 2,5-bis (hydroxymethyl)furan used as chain extender, the fibers can undergo Diels-Alder reaction with dienophile-containing molecule. In this specific case, two maleimide-containing compounds were used as functionalizing agent. Furthermore, the polyurethane nanofibers have been proven to be biocompatible. The facile and quantitative synthesis, the ease of spinnability, the biocompatibility, together with the good mechanical properties and the functionalization rapidity and reversibility make this polymer an interesting material in a wide range of applications from the tissue engineering to the biomolecular immobilization.

Author contributions

The manuscript was written through contributions of all authors. All authors have given approval to the final version of the manuscript.

Data availability

The raw data required to reproduce these findings are available by the corresponding author upon request.

Declaration of Competing Interest

The authors declare no competing financial interest.

Acknowledgment

Financial support from the University of the Basque Country (UPV/EHU) (GIU18/216 and GIU 19/088 Research Groups), from the Council of Gipuzkoa (2020-CIEN-000092-01), from the Basque Country Government (PIBA-2020-1-0041, KK-2020-00053) and from Spanish Ministry of Science, Innovation and Universities and European Union (MICINN/EU/FEDER) in the frame of PID2019-105090RB-I00 project and financial support from the Basque Country Government in the frame of Grupos Consolidados (IT-1690-22) are gratefully acknowledged. Moreover, we are grateful to the Macrobehavior-Mesostructure-Nanotechnology, Electronic Microscopy and Material Microanalysis and NMR Services SGIker units of the UPV/EHU. Stefano Torresi wishes to acknowledge the Ministry of Science and Innovation for his PhD grant (PRE2020-092538).

Appendix A. Supplementary data

^{1}H-NMR of the two polyurethane films and spectra of the DA performed after the r-DA. Supplementary data to this article can be found online at https://doi.org/10.1016/j.reactfunctpolym.2022.105353.

References

[1] J. Fang, H. Niu, T. Lin, X. Wang, Applications of electrospun nanofibers, Chin. Sci. Bull. 53 (15) (2008) 2265–2286.
[2] X. Wang, B.S. Hsiao, Electrospun nanofiber membranes, Curr. Opin. Chem. Eng. 12 (2016) 62–81.

[3] S. Liao, B. Li, Z. Ma, H. Wei, C. Chan, S. Ramakrishna, Biomimetic electrospun nanofibers for tissue regeneration, Biomed. Mater. 1 (3) (2006) R45–R53.
[4] L. Min, Z. Yuan, L. Zhong, Q. Liu, R. Wu, Y. Zheng, Preparation of chitosan based electrospun nanofiber membrane and its adsorptive removal of arsenate from aqueous solution, Chem. Eng. J. 267 (2015) 132–141.
[5] J.H. Lee, S.H. Park, S.H. Kim, Fabrication of bio-based polyurethane nanofibers incorporated with a triclosan/cyclodextrin complex for antibacterial applications, RSC Adv. 10 (6) (2020) 3450–3458.
[6] E. Sancak, R. Erdem, Functionalization techniques for electrospun nanofibers for drug delivery applications: a review, Usak Univ. J. Mater. Sci. 3 (2014) 180.
[7] E. Blasco, M.B. Sims, A.S. Goldmann, B.S. Sumerlin, C. Barner-Kowollik, 50th anniversary perspective: polymer functionalization, Macromolecules. 50 (14) (2017) 5215–5252.
[8] Q. Shi, X. Chen, T. Lu, X. Jing, The immobilization of proteins on biodegradable polymer fibers via click chemistry, Biomaterials. 29 (8) (2008) 1118–1126.
[9] H. Yang, Q. Zhang, B. Lin, G. Fu, X. Zhang, L. Guo, Thermo-sensitive electrospun fibers prepared by a sequential thiol-ene click chemistry approach, J. Polym. Sci. A Polym. Chem. 50 (20) (2012) 4182–4190.
[10] J. Funel, S. Abele, Industrial applications of the Diels–Alder reaction, Angew. Chem. Int. Ed. 52 (14) (2013) 3822–3863.
[11] C. Chang, Y. Liu, Functionalization of multi-walled carbon nanotubes with furan and maleimide compounds through Diels–Alder cycloaddition, Carbon. 47 (13) (2009) 3041–3049.
[12] O. Kalaoglu-Altan, A. Kirac-Aydin, B. Sumer Bolu, R. Sanyal, A. Sanyal, Diels–Alder "Clickable" biodegradable nanofibers: benign tailoring of scaffolds for biomolecular immobilization and cell growth, Bioconjug. Chem. 28 (9) (2017) 2420–2428.
[13] B. Willocq, F. Khelifa, J. Brancart, G. Van Assche, P. Dubois, Raquez J-., One-component Diels–Alder based polyurethanes: a unique way to self-heal, RSC Adv. 7 (76) (2017) 48047–48053.
[14] P. Tanasi, M. Hernández Santana, J. Carretero-González, R. Verdejo, M.A. López-Manchado, Thermo-reversible crosslinked natural rubber: a Diels-Alder route for reuse and self-healing properties in elastomers, Polymer. 175 (2019) 15–24.
[15] K. Luo, G. Song, Y. Wang, J. Yu, J. Zhu, Z. Hu, Low-k and recyclable high-performance POSS/polyamide composites based on Diels–Alder reaction, ACS Appl. Polym. Mater. 1 (5) (2019) 944–952.
[16] V. Froidevaux, M. Borne, E. Laborbe, R. Auvergne, A. Gandini, B. Boutevin, Study of the Diels–Alder and retro-Diels–Alder reaction between furan derivatives and maleimide for the creation of new materials, RSC Adv. 5 (47) (2015) 37742–37754.
[17] A. Gandini, The furan/maleimide Diels–Alder reaction: A versatile click–unclick tool in macromolecular synthesis, Prog. Polym. Sci. 38 (1) (2013) 1–29.
[18] A. Saralegi, L. Rueda, B. Fernández-d'Arlas, I. Mondragon, A. Eceiza, M. A. Corcuera, Thermoplastic polyurethanes from renewable resources: effect of soft segment chemical structure and molecular weight on morphology and final properties, Polym. Int. 62 (1) (2013) 106–115.
[19] C. García-Astrain, K. González, T. Gurrea, O. Guaresti, I. Algar, A. Eceiza, et al., Maleimide-grafted cellulose nanocrystals as cross-linkers for bionanocomposite hydrogels, Carbohydr. Polym. 149 (2016) 94–101.
[20] C. Oh, E.H. Choi, E.J. Choi, T. Premkumar, C. Song, Facile solid-state mechanochemical synthesis of eco-friendly thermoplastic polyurethanes and copolymers using a biomass-derived furan diol, ACS Sustain. Chem. Eng. 8 (11) (2020) 4400–4406.
[21] T. Calvo-Correas, A. Santamaria-Echart, A. Saralegi, L. Martin, Á. Valea, M. A. Corcuera, et al., Thermally-responsive biopolyurethanes from a biobased diisocyanate, Eur. Polym. J. 70 (2015) 173–185.
[22] C.B. Smith, The infrared spectroscopy of alkenes, Spectroscopy. 31 (11) (2016 Nov 1) 28–34.
[23] L. Ugarte, B. Fernández-d'Arlas, A. Valea, M.L. González, M.A. Corcuera, A. Eceiza, Morphology–properties relationship in high-renewable content polyurethanes, Polym. Eng. Sci. 54 (10) (2014) 2282–2291.
[24] B. Fernández d'Arlas, L. Rueda, K. de la Caba, I. Mondragon, A. Eceiza, Microdomain composition and properties differences of biodegradable polyurethanes based on MDI and HDI, Polym. Eng. Sci. 48 (3) (2008) 519–529.
[25] D.K. Chattopadhyay, D.C. Webster, Thermal stability and flame retardancy of polyurethanes, Prog. Polym. Sci. 34 (10) (2009) 1068–1133.
[26] Z. Mou, S. Feng, E.Y.X. Chen, Bio-based difuranic polyol monomers and their derived linear and cross-linked polyurethanes, Polym. Chem. 7 (8) (2016) 1593–1602.
[27] J. Choi, D.S. Moon, J.U. Jang, W.B. Yin, B. Lee, K.J. Lee, Synthesis of highly functionalized thermoplastic polyurethanes and their potential applications, Polymer. 116 (2017) 287–294.
[28] C. Altinkok, H.R.F. Karabulut, M.A. Tasdelen, G. Acik, Bile acid bearing poly (vinyl chloride) nanofibers by combination of CuAAC click chemistry and electrospinning process, Mater. Today Commun. 25 (2020), 101425.
[29] R. Moradi, J. Karimi-Sabet, M. Shariaty-Niassar, M.A. Koochaki, Preparation and characterization of polyvinylidene fluoride/graphene Superhydrophobic fibrous films, Polymers. 7 (8) (2015).
[30] International Organization for Standardization, ISO 10993-5. Biological Evaluation of Medical Devices. Test for In Vitro Cytotoxicity, 2009.
[31] Y. Oz, A. Sanyal, The taming of the Maleimide: fabrication of Maleimide-containing 'clickable' polymeric materials, Chem. Rec. 18 (6) (2018) 570–586.
[32] E. Vivès, B. Lebleu, One-pot labeling and purification of peptides and proteins with fluorescein maleimide, Tetrahedron Lett. 44 (29) (2003) 5389–5391.
[33] X. Liu, P. Du, L. Liu, Z. Zheng, X. Wang, T. Joncheray, et al., Kinetic study of Diels–Alder reaction involving in maleimide–furan compounds and linear polyurethane, Polym. Bull. 70 (8) (2013) 2319–2335.
[34] A. Gandini, D. Coelho, M. Gomes, B. Reis, A. Silvestre, Materials from renewable resources based on furan monomers and furan chemistry: work in progress, J. Mater. Chem. 19 (45) (2009) 8656–8664.
[35] A. Gandini, A. Silvestre, D. Coelho, Reversible click chemistry at the service of macromolecular materials. Part 4: Diels–Alder non-linear polycondensations involving polyfunctional furan and maleimide monomers, Polym. Chem. 4 (5) (2013) 1364–1371.